

Advancements in Oncological Dynamic Contrast-Enhanced Mri: A Review and Critical Analysis of Prior Studies

Faizan Farooq¹, Mohit Sharma¹, Khursheed Ahmad¹, Srishti Bhardwaj¹ and Arti²

¹ Department of Allied Health Sciences, ¹ Chitkara School of Health Sciences, Chitkara University, Punjab

² Department of Life Sciences Rayat Bahra University, Punjab-140103

DOI : <https://doi.org/10.51583/IJLTEMAS.2025.1412000010>

Received: 13 December 2025; Accepted: 19 December 2025; Published: 26 December 2025

ABSTRACT

Dynamic contrast-enhanced magnetic-resonance imaging(DCE-MRI) has emerged as a transformative method in oncological imaging, contributing to findings on tumor vascularity, permeability, and treatment response. This review outlines an extensive assessment of DCE-MRI implementation across various malignancies, with a specific emphasis on liver tumors, spinal metastases, and breast cancer. Through examination key pharmacokinetic parameter such as Ktrans, Ve and Kep, the article highlights their diagnostic and prognostic value in discriminating lesion types and forecasting microvascular invasion. It also delves into the integration of artificial intelligence and radiomics in optimizing the interpretability and reproducibility of DCE-MRI data. The review confronts issues related to motion artifacts, regulation, and crossplatform variability, while recommending future directions or clinical uptake and research evolution. Through this synthesis, DCE-MRI is placed as a crucial tool in precision oncology, with the extension of implementation across anatomical systems.

Key Words: Dynamic contrast-enhanced magnetic contrast resonance imaging (DCE-MRI), forward volume transfer (Ktrans), reverse constant (Kep), Computed tomography (CT) and extravascular extracellular space volume fraction (VeVe)

INTRODUCTION

An operational imaging approach, Dynamic Contrast-Enhanced Magnetic Resonance imaging (DCE-MRI) that facilitates neumarical evaluation of blood flow, tissue perfusion, and vascularity by examining signal refinement curves subsequent to contrast administration [1]. This approach records dynamic shifts in tumor vascularity permeability, often influenced by antiangiogenic therapies, delivering pivotal revelations into tumor biology and response to treatment [2]. DCE-MRI creates Pharmacokinetic variables such as the forward volume transfer (Ktrans), reverse constant (Kep), and extravascular extracellular space volume fraction (Ve), each indicating distinct elements of the tumor microenvironment and vascular behavior. These parameters facilitate monitoring of therapeutic effectiveness [3]. DCE-MRI proposes superior sensitivity than conventional MRI in recognizing subtle changes within the tumor microenvironment, leading to a significant early biomarker of treatment response [4]. This approach assists in voxel-wise calculations of perfusion characteristics, facilitating exact outlining of tumor heterogeneity and permitting personalized treatment strategies. Clinically-MRI has shown utility in multiple cancer: in hepatocellular carcinoma (HCC), it assists in assessing microvascular invasion (MVI) and distinguishing HCC from hepatic adenomas; in cervical cancers, it elevates diagnostic confidence and help avoid unnecessary radical surgeries [5]. and in soft tissue tumors, combined multiparametric analysis with diffusion imaging have diagnostic accuracy [6]. Furthermore, quantitative parameters such as Ktrans, Kvp, Ve, and add to tumor sorting and upgrade early prediction of treatment failure and recurrence risk [7]. Elevated Ktrans values are often associated with increased vascular permeability characteristic of malignant tumors, while higher Kep can reflect aggressive tumor behavior and enhanced perfusion [8,9]. Increased Ve typically indicates tumors with extensive extracellular matrix or edema, suggesting potential for aggressive spread [5]. These capabilities, such as planning and adaptive radiotherapy, enhance precision in tumor targeting [10].

Ultrasound has a low sensitivity for early (HCC), generally varying from 60% to 70% which can significantly obstruct identification. Additionally, the results could be fluctuating due to operator-dependent factors, resulting in unpredictable findings [9]. Computed tomography (CT) demonstrates balanced specificity for HCC detection, generally between 70% and 80%. This limitation is aggravated by the risk related to ionizing radiation effects, particularly troubling patients who require frequent imaging due to high risk of reappearance [8].

Standard MRI is vulnerable to motion distortion, notably those done by patient breathing, which can compromise image quality. Furthermore, its precision declines when assessing small lesions, making it less effective in identifying early-stage HCC. DCE-MRI offers numerical analysis, such as Ktrans which reflect the measure of contrast agent transfer out of blood vessels within the extracellular medium. This parameter is vital to distinguish benign and malignant tumors which generally exhibit higher Ktrans values because of elevated vascular permeability and blood dynamics [9].

DCE-MRI offers quantitative evaluations of vascular characteristics, which are crucial for understanding tumor microenvironments and hemodynamics, thus elevating tumor characterization compared to standard MRI techniques [11]. The technique's ability to assess tumor vascularity and permeability provides insights into tumor behavior, which is key to therapeutic planning and enhancing patients result [12]. DCE-MRI can also facilitate the differentiation of malignant and benign tumors by sharing elaborated findings of tumor blood flow, which is often challenging with conventional imaging [13]. DCE-MRI can detect changes in tumor vascularity and microenvironment, providing critical insights that reduce the need for invasive biopsies in assessing response to therapy [14].

This investigation seeks to examine the reliability of (DCE-MRI) in categorizing benign and malignant liver tumors with precision, enhancing noninvasive diagnostic capabilities. DCE-MRI has shown potential in providing detailed predictions of microvascular invasion (MVI) and vascular encapsulation tumor clusters (VETC) in HCC, attaining the

area under the curve (AUC) of 0.85 in internal validation [9]. The integration of clinical and radiomics models in DCE - MRI can improve diagnostic performance, offering a non-surgical substitute to traditional biopsy methods. However, variability in imaging protocols and the need for standardization remain challenges that could affect the clinical application of DCE-MRI, Building upon these foundations, this review aims to objectively examine the breakthrough and clinical implementation of dynamic contrast-enhanced MRI in oncological imaging. By weaving together contemporary publications on DCE-MRI's diagnostic, prognostic and therapeutic tracking mechanisms involving numerous tumor categories such as liver, spinal and breast cancerous conditions.

Technical Foundation of DCE-MRI

A valuable means of evaluating tumor vascularity by quantifying how contrast agents move through tissue compartments is offered by (DCE-MRI) Dynamic contrast-enhanced MRI. Perfusion rate at which contrast material transitions from the blood flow dynamics vessels into the extracellular matrix is described through one key parameter, Ktrans (volume transfer constant), both blood flow and the permeability of vessel walls is reflected by this rate. To calculate Ktrans the TTofts model, which underpins many DCE-MRI analyses, treats tissue as two interacting compartments and uses an arterial input function. Higher tumor aggressiveness and indication of how the tumor might respond to therapies are often linked to elevated Ktrans [15,16].

Kep (rate constant), another crucial metric, exposes how quickly the contrast agent returns from the extracellular matrix back into the bloodstream. Kep is typically computed as Ktrans divided by Ve (the volume of the extracellular space). It provides insights into the efficacy of contrast clearance and highlights differences in vascular permeability between tumor types [17,18]. As shown in Figure 1, ...

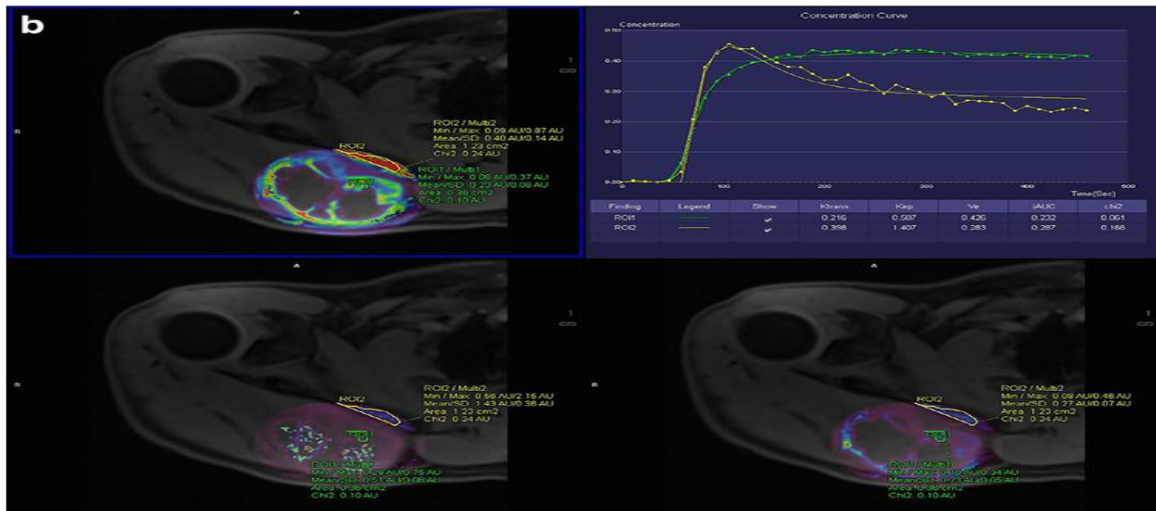


Fig 1. The values included are k_{trans} (0.398 min⁻¹), K_{ep} (1.407 min⁻¹), V_e (0.98), and $iAUC$ observed in the ROI was labelled as type IV on the basis of tissue contrast kinetics.

$$\text{Formula: } \left\{ K_{Trans} = \frac{K_{ep} \cdot V_e}{V_p} \right\} \dots \dots \dots (1)$$

The parameter V_e (extracellular volume fraction) measures the proportion of tissue volume occupied by the extracellular space. Tumors with higher V_e values have larger extracellular areas due to factors like edema or a loose extracellular matrix, features often seen in more aggressive malignancies [18,19].

$$\text{Formula: } \left\{ K_{ep} = \frac{K_{Trans}}{V_e} \right\} \dots \dots \dots (2)$$

Collectively, K_{trans} , K_{ep} , and V_e help assess key features of tumor biology, including angiogenic, perfusion, and vascular leakiness. High K_{trans} and K_{ep} values generally point to active tumor growth and rich blood supply, while lower levels may suggest necrosis or poor vascularization. These parameters are critical in predicting tumor behavior and potential treatment responses. Its important to note that accurate measurements of these parameters can be affected by several technical factors. Motion during imaging, especially due to breathing, can distort time-intensity data. Additionally, inconsistencies in contrast agent dosing, timing of scans, or the choice of input functions can lead to variability in results. Standardizing imaging protocols and addressing motion artifacts remain essential for reliable DCE-MRI analysis. [2,15]. As demonstrated in Figure 2

$$\text{Formula: } \left\{ V_e = \frac{K_{Trans}}{K_{ep}} \right\} \dots \dots \dots (3)$$

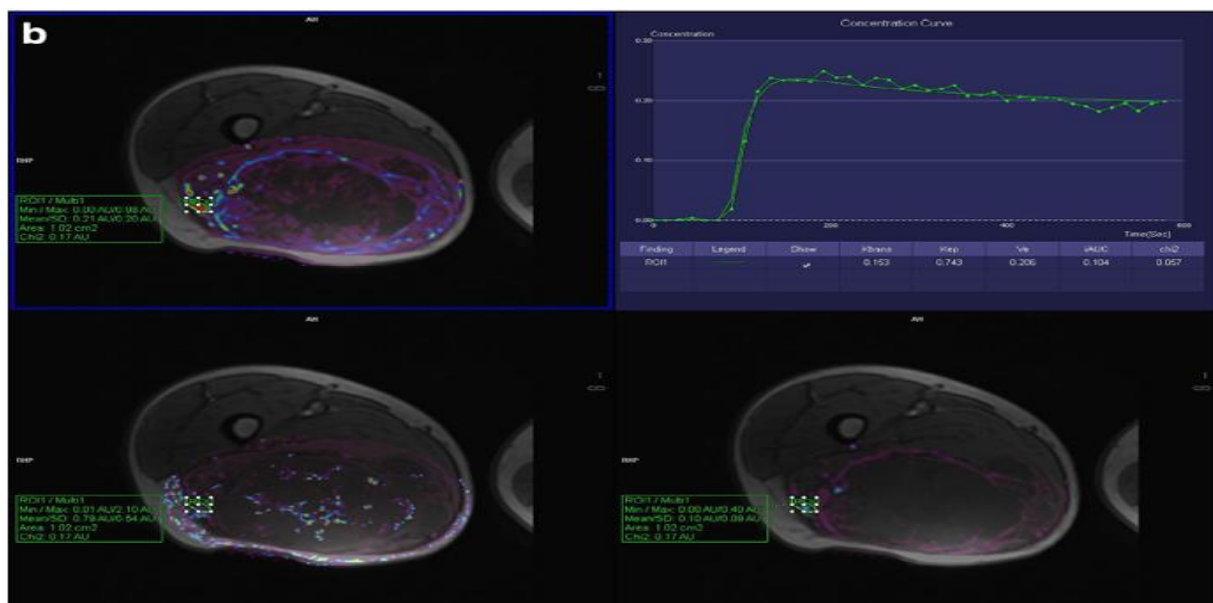


Fig 2. DCE-MRI outcomes in a 48-year-old male show low K_{trans} , K_{ep} , V_e , and $iAUC$ values within a constrained ROI, with a type III tissue contrast concentration curve.

METHODOLOGY

This review was carried out using an arranged literature search framework following established narrative review methodology. Validated investigations examining dynamic contrast-enhanced MRI, pharmacokinetic modeling, and quantitative parameters such as K_{trans} , K_{ep} , V_e and V_p in liver tumor cancer were recognized by PubMed, Scopus, Google Scholar and ScienceDirect. The search included articles published from 1998 to 2025 using multiple keywords. Inclusion criteria were, Studies involving DCE-MRI quantitative analysis, articles using Tofts, Extended Tofts, or advanced Pharmacokinetic models, studies recognized PK parameters with tumor grade, vascularity, or clinical efficacy. Conference abstracts, non-pharmacokinetic studies, and articles lacking quantitative assessment were excluded. Data from each study were gathered relating to methodology, PK parameters used, diagnostic efficiency, strengths, and limitations to integrate patterns, verify gaps, and showcase future research pathways.

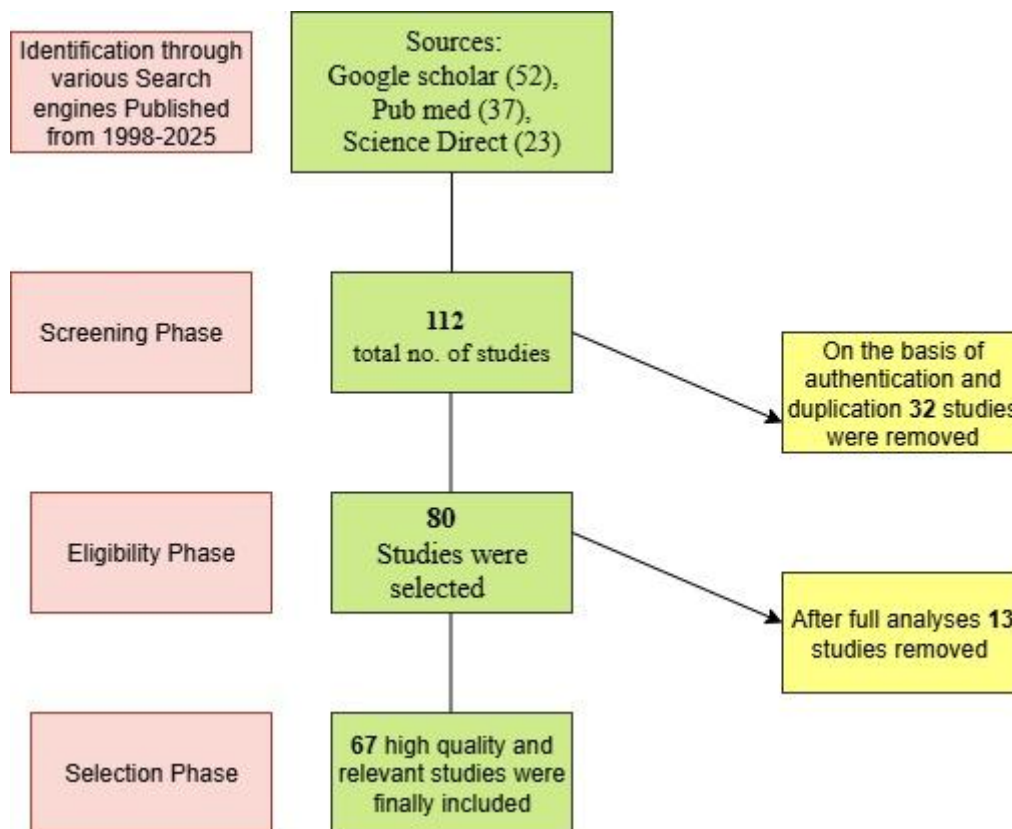


Fig 3: Representing preferred reporting items for systematic reviews and meta-analyses (PRISMA) for methodology

Diagnostic Applications of DCE-MRI

Diagnostic work of DCE-MRI in Differentiating Benign vs. Malignant Liver Lesions

In a regular clinical approach, it is rare to come across obstacles when trying to separate benign from malignant soft tissue tumors utilizing standard MRI alone, due to intersecting morphological features and signal levels [20]. Latest progress, including diffusion-weighted imaging (DWI), specifically with intravoxel incoherent motion (IVIM) structuring, has enabled improved distinction by examining water diffusion traits [21]. Parameters like the apparent diffusion coefficient (ADC), pure diffusion coefficient (D), Pseudodiffusion coefficient (D), and perfusion fraction (f) help distinguish true diffusion from perfusion-linked effects [22]. These techniques have shown capability in improving tumor profiling. Supportively, DCE-MRI relates pharmacokinetic simulating (e.g., Tofts model) to extract parameters like K_{trans} , K_{ep} , and V_e , and semi-quantitative metrics such as I_{auc} , providing additional operational understandings to aid in tumor separation with studies reporting significantly higher K_{trans} values in HCC, reflecting its aggressive angiogenesis and greater microvascular permeability [13]. with reported area under the curve (AUC) values of 1.0 during validation and 0.8 in final test

phases, confirming their potential for clinical application [23]. Support vector machine (SVM)-based approaches have yielded detection rate and precision around 84% and 81% respectively, in classifying liver lesions, reinforcing DCE-MRI's diagnostic value.

Table 1. Summary of key methodological parameters from selected studies evaluating dynamic contrast-enhanced MRI in oncologic imaging, including MRI field strength, contrast agent protocols, computational analysis tools, pharmacokinetic models, assessed dynamic variables, and pre-/post-treatment timing.

Study year	Tesla MRI	Radiologic tracer	Computational analysis	numerical analysis	Reviewed Dynamic study variables,	Duration assessment: Dynamic MRI variables
Chu et al [24]. 2013.	1.5 Tesla MRI	Gd-DTPA was injected intravenously at 0.1mmol/kg with an infusion rate of 2.5 ml	NordicICE version 2.3 (NordicNeuroLab)	Tofts-based dual-compartment kinetic framework	Vp, Ktrans, AUC, PE	Pre-therapy 2-115 days; post-treatment 0-187 days
Spratt et al [25, 26].	1.5 Tesla MRI	Gadolinium-DTPA was administered intravenously at 0.1 mmol/kg using volumetric flow rate at 2 & e ml/s	NordicICE (Nordic NeuroLab)	Tofts 2-compartment pharmacokinetic model	Vp, Ktrans,	Fifty-seven days after therapy (IQR, 51-62 days).
Kumar et al. [27], 2017	1.5 Tesla MRI	Gd- contrast agent 0.1 mmol/kg at a controlled injection speed of 2-3 ml/s	NordicICE version 2.3 (NordicNeuroLab)	Expanded dual-compartment adopted from the original Tofts approach	Vp, Ktrans	Pre and post are not specified
Lis et al. [28], 2017	1.5 Tesla MRI	The contrast agent gadolinium 0.1 mmol/kg fluid transfer unit 2.5 ml/s	NordicICE (NordicNeuroLab) and MATLAB (Mathworks)	Toft's pharmacokinetic model analysis	Vp, Ktrans	1 hour prior to and following therapy, as opposed to later phases (range, 51-504 days)
Chen et al. [15], 2021	3T MRI	Gadopentetate dimeglumine 0.1 mmol/kg, throughput of 2 ml/s	GE ADW4.6 workstation and GenIQ software	Extended Toft's 2-compartment pharmacokinetic model	Ktrans, Kep, Ve	1 week prior to therapy; 1/3 months post-therapy

Chung et al. Assessed the clinical performance of conventional MRI in distinguishing benign from malignant soft tissue tumors by assessing parameters like lesion depth, size, and signal heterogeneity. Their approach yielded a detection rate of 64%, a precision of 85%, and an overall diagnostic precision of 77%. When compared to findings from more recent studies employing multiparametric MRI, it is evident that incorporating multiple imaging parameters enhances diagnostic precision. For instance, studies report improvements in sensitivity from 71% to 81 % while maintaining constant specificity (69% to 83%) and precision [25].

Hu et al. Has proven the possibility of utilizing radiomics-based machine learning to separate benign and malignant soft tissue neoplasms. In their study, least absolute shrinkage and selection operator (LASSO) logistic regression frameworks built on apparent diffusion coefficient (ADC) traits accomplished superior diagnostic correctness (AUC=0.955, sensitivity = 83%, specificity = 100%) compared to those according to fat-suppressed T2WI attributes

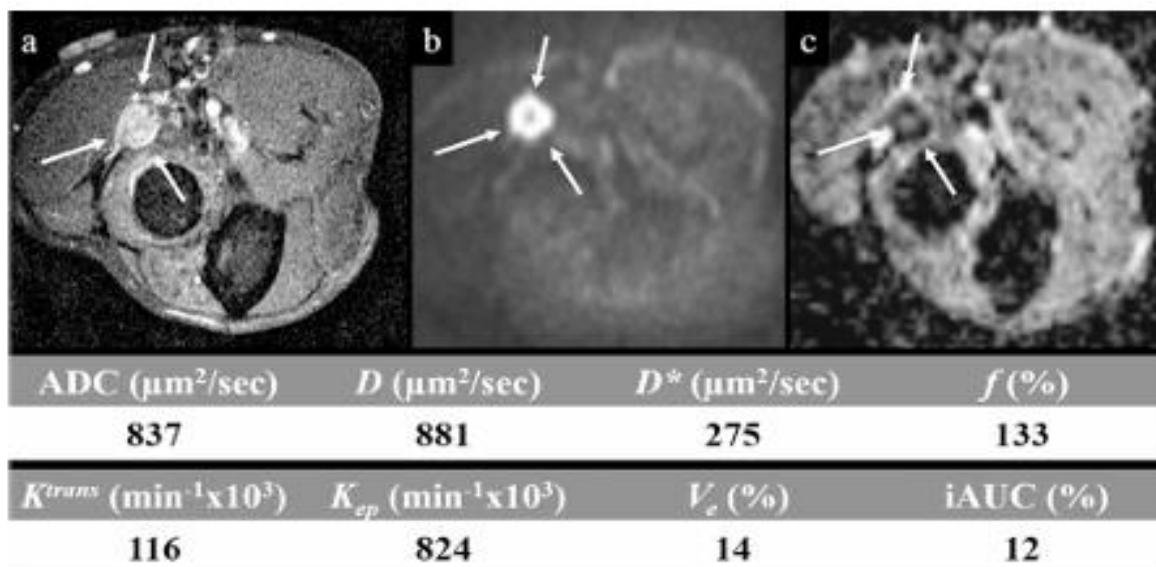


Fig 4: Multiparametric MRI including IVIM-DWI and DCE-MRI indicates a malignant soft tissue neoplasm, later confirmed as myeloid sarcoma. Imaging metrics such as ADC, IVIM, and perfusion parameters support the diagnosis.

(AUC = 0.75). Pattern attributes such as mean ADC, HISTO-skewness, and GLCM-associated metrics recorded slight variations in tissue heterogeneity. Significantly, benign tumors had negatively skewed ADC histograms, while malignant lesions were positively skewed due to elevated cellularity. Their application of whole-tumor volumetric division and replicable feature derivation using LIFEx software supports the methodological effectiveness of radiomics in this background. These outcomes offer convincing proof that ADC-based radiomics systems, when integrated with machine learning algorithms like LASSO, can efficiently identify tumor types, providing potential clinical decision assistance tools with high accuracy [29].

Quantitative assessment from intravoxel incoherent motion DWI (IVIM-DWI) and dynamic contrast-enhanced MRI (DCE-MRI) both suggested a malignant soft tissue neoplasm. Histopathological confirmation identified the lesion as myeloid sarcoma. Panel D summarizes the results from the multiparametric MRI analysis, including metrics such as ADC, IVIM, and perfusion-based parameters supporting the final diagnosis.

Key diffusion metrics, for example, the (ADC) apparent diffusion coefficient and the diffusion coefficient (D), have demonstrated statistically appropriate differences among benign and malignant tumors [12]. While D is expected to perform ADC due to its reduced sensitivity to perfusion-related effects and improved reflection of true tissue diffusivity, receiver operating characteristic (ROC) analysis showed comparable diagnostic utility between the two (AUC values of 0.752 for ADC and 0.742 for D) [30]. These observations align with findings from Lim et al who noted significant differentiation using D but not ADC. Discrepancies may be differences in imaging technique, including Rijswijk's use of a 1.5 T scanner with limited b-values in early IVIM-DWI [13,6] Additionally, recent hypotheses propose that benign tumors might exhibit more heterogeneous or pronounced

microcapillary perfusion than malignant ones, contributing to the lack of significant differences in D and perfusion fraction (f) between tumor types. This notion is supported by multiparametric MRI in improving soft tissue tumor evaluation while also acknowledging the limitations of perfusion-sensitive indices in certain tumor contexts [13]. Subset evaluation in the same study uncovered that IVIM-DWI was restricted in separating benign from malignant myxoid tumors because of intersecting ADC figures, resulting in extracellular matrix fluctuation [31]. Yet, DCE-MRI factors such as K_{trans} and IAUC persisted significantly different even in these difficult scenarios, validating the benefit of perfusion imaging in tumors with high myxoid information. This showcases the relevance of adjusting the imaging method based on tumor structure [7].

Prediction of Microvascular invasion (MVI)

DCE-MRI combined with radiomics has advanced presurgical estimation of MVI in HCC. Models incorporating intratumorally and peritumoral features have achieved validation AUCs as high as 0.879, understanding their potential for improving surgical planning [22]. Other studies using contrast agents such as Gd-EOB-DTPA have further highlighted the role of MRI-derived radiomics in guiding clinical decisions related to MVI risk [32].

[33], Feng conducted a study and set a goal to produce and authenticate an integrated internal tumor region and tumor margin radiomics framework to forecast MVI before surgery for initial HCC cases that applied gadolinium-ethoxy benzyl-diethylenetriamine (Gd-EOB-DTPA) improved MRI. One hundred and ten HCC cases took part in this investigation. They had a presurgical and curative hepatectomy, Gd-EOB-DTPA advanced MRI analysis, and 40.0 % & 38.2% of the subjects were Microvascular invasion affirmative forecasting framework. By its precise specificity, sensitivity, and AUC, the integrated peritumoral & intratumoral radiomics model facilitated doctors in forming reliable treatment moves pre-surgery [31]. Another article by [34]. by implementation of radiomics-based nomograms for 356 cases with solitary HCC < 5cm, Microvascular Invasion, and reappearance-free survival (RFS) was estimated. During verification, it has been observed that 0.879 was the cohort AUC of the MVI nomogram by logistic regression observations and 0.920 by random forest. The median RFS of 30.5 months and >96.9 months, in corresponding order, were observed in patients with an MVI. Return was autonomously estimated by age, histologic MVI, alkaline phosphatase, and alanine aminotransferase, with an AUC of 0.654 in the RFS endorsement cohort [21]. DCE-MRI combined with radiomics has advanced the pre-surgical evaluation of MVI in HCC. Models incorporating intratumorally and peritumoral features have achieved validation AUCs as high as 0.879, understanding their potential for improving surgical planning [31]. Other studies using contrast agents such as Gd-EOB-DTPA have further highlighted the role of MRI-derived radiomics in guiding clinical decisions related to MVI risk [21].

Another study conducted by Kumar et al. In which he investigated the differentiation in duration to reappearance identification between present time MRI and DCE-MRI. Localized reappearance about 18 months prior to traditional MRI in five patients was detected by DCE-MRI (mean \pm standard deviation, 6.6 ± 6.8 months) [28]. revealed that the V_p variable could identify effective reaction to therapy within 10 days post-intervention, which was likely too early than traditional MRI. DCE-MRI varies subsequent to RT could anticipate tumor reaction in less than 6 months, to evaluate the point of tumor steadiness that is approximately half the period essential by standard MRI.

DCE-MRI in other Cancers

Beyond liver cancers, DCE-MRI has been applied in breast cancer, where radiomics models based on DCE features have achieved AUCs of 0.89 for differentiating benign and malignant lesions using SVM classifiers. In cervical cancers, DCE-MRI's semi-quantitative parameters have shown strong sensitivity and specificity for malignancy detection, although some limitations persist in distinguishing among all tumor types [35].

DCE-MRI in the evaluation of spinal Metastases

Spinal metastases affect 40-70% of advanced cancer patients and are a major source of morbidity due to pain, paralysis, and vertebral fractures. Radiotherapy is a common treatment; however, conventional methods have shown limited ability to assess post-treatment MRI changes, as nearly half of lesions may appear unchanged despite clinical response. DCE-MRI has emerged as a superior modality in this context, offering kinetic

parameters such as K_{trans} , V_e , and V_p , which reflect changes in vascular permeability and interstitial fluid space. These biomarkers are highly sensitive to angiogenic and cytotoxic responses, allowing earlier detection, like RECIST. Several studies report that DCE-MRI can distinguish responders from non-responders at much earlier time points after stereotactic body radiotherapy (SBRT) or CyberKnife therapy. This has important implications for guiding timely salvage therapies and optimizing patient outcomes. However, small sample sizes remain a limiting factor in many spinal metastasis DCE studies, indicating the need for larger-scale prospective trials. [14,21]

Therapeutic Monitoring with DCE-MRI

Fluctuation in DCE-MRI criteria and Analysis of tumor outcome after Radiation Therapy

Numerous studies have explored the potential of DCE-MRI parameters particularly, K_{trans} , V_p , and V_e , to monitor tumor response to radiation therapy (RT). In a study by Spratt et al., 2016 a marked reduction in k_{trans} was observed approximately two months following stereotactic body radiotherapy (SBRT). Specifically, up to 75% of pathologies showed a decline in mean k_{trans} , with some tumors demonstrating a reduction of up to 92%. Interestingly, in one patient who experienced local recurrence, k_{trans} values actually increased. However, due to a limited sample size, statistical comparison between responders and non-responders were not feasible. Kumar et al. provided more definitive results, reporting a significant difference in k_{trans} reduction among treatment effective and ineffective groups (-66% vs. -7%, $p = 0.01$), with no local recurrence observed in patients who achieved the more substantial k_{trans} drop [27]. Lis et al. evaluated early responses in six patients with spinal metastasis undergoing high-dose image-guided radiotherapy (HD IGRT). They found a median reduction in k_{trans} from 4.84 to 2.3 within one-hour post-treatment. No progression was observed during a follow-up period extending over a period of 839 days [15]. Similarly, [15] documented that responders demonstrated an average k_{trans} reduction of -32.6%, while non-responders demonstrated an average k_{trans} reduction of -32.6%, while non-responders showed a median increase of +20.4% ($p = 0.001$). In contrast, (Chu et al., 2013) did not observe statistically significant changes in k_{trans} following RT ($p = 0.48$), possibly due to differences in timing or methodology [31].

(VP) For the plasma volume parameter, Li et al. found a rapid 65.2% reduction in median V_p one-hour post-HD IGRT, a finding mirrored by Spratt et al. who documented a 58.7% decrease in spinal sarcomas post-SBRT. Chu et al. highlighted the predictive value of V_p , showing a notable change in V_p changes among treatment effective groups (-65.66%) and ineffective groups (+145.27%+206.79%), while Kumar et al. corroborated this with a -76% versus +30% difference ($p = 0.01$) [30]. (VE) In contrast, this parameter showed inconsistent trends. Vellayappan's study reported no statistically significant changes in V_e values over time post-SBRT [36], found a mean increase of 161.9% on V_e five weeks post-RT. Despite this, no marked disparity were observed among effective treatment groups and non-effective groups in V_e levels or percentage changes. [37]. These findings that K_{trans} and V_p are more reliable indicators of early therapeutic response to RT in liver and metastatic tumors than V_e . However, variations across studies related to timing, tumor type, and imaging protocols highlight the need for standardized methodologies to fully leverage DCE-MRI for treatment monitoring.

DCE-MRI, Gd-DTPA, gadolinium-diethylenetriamine Penta acetic acid; V_p proportion of tissue volume occupied by blood plasma; K_{trans} , constant representing the movement rate among blood plasma and extracellular matrix; AUC, total signal intensity change over time; PE-maximum contrast enhancement observed; IQR, interquartile span; V_e , extravascular extracellular space volume fractions; (PS) permeability surface product; CT, RT, radiation therapy [38].

Comparative Performance of DCE-MRI

DCE-MRI offers several advantages over conventional imaging modalities. It provides higher sensitivity than ultrasound, which is known for its lower sensitivity and operator dependency [35]. Compared to CT, DCE-MRI avoids ionizing radiation and offers superior specificity [31]. Moreover, it mitigates motion artifacts seen in standard MRI and improves the detection of smaller lesions, which is crucial for early diagnosis [33]. DCE-MRI is an important tool in assessing therapeutic response. Changes in K_{trans} after treatments, particularly for HCC, can reflect shifts in tumor blood flow and permeability, offering early indications of response to ablative or

systemic therapies [34]. Significant reductions in Ktrans have been correlated with superior progression-free survival (PFS) and overall survival (OS), showcasing its prognostic value [39]. Quantitative DCE-MRI models also contribute to predicting microvascular invasion in early-stage HCC, aiding in the recognition of patients at greater vulnerability of recurrence [34]. Although data on prostate cancers are more limited, DCE-MRI is widely recognized for its broader role in monitoring vascularity and treatment responses across various tumor types [40].

Table 2. Output evaluation among FS-T2WI-based and ADC-based Radiomics system of identifying Soft tissue Neoplasms

Parameter	--	P=0.017 (vs.FS-T2WI)
Statistical Significance	0.750	0.955
Accuracy	70.8%	91.7%
Specificity	96.0%	100.0%
Sensitivity	55.0%	83.3%
AUC (Validation)	FS-T2WI Model	ADC-Based Model
Feature Types used	Texture features (GLCM, GLZLM) from FS-T2WI	Texture+Histogram (e.g.,HISTO-skewness) from ADC
Modeling method	LASSO- Logistic Regression	LASSO-Logistic Regression

In a straightforward analysis study, Hu et al. assessed radiomics-derived machine learning frameworks obtained from fat-suppressed T2-weighted imaging (FS-T2WI) and apparent diffusion coefficient (ADC) maps to differentiate benign and malignant soft tissue neoplasms [29]. Utilizing LASSO-logistic regression, the ADC-grounded design exhibited meaningfully superior diagnostic capability, reaching an AUC of 0.955 in the verification cohort, with a sensitivity of 83%, a specificity of 100% and overall accuracy of 91.7%. In contrast, the FS-T2WI framework generated reduced sensitivity (55%) and accuracy (70.8%), even though preserving high specificity. The variation in AUC among the models was quantitatively notable (P=0.017), highlighting the more effective identifying power of ADC extracted pattern traits. These outcomes revealed the diagnostic benefit of diffusion-based radiomics models over conventional T2-weighted imaging, specifically when volumetric examination and higher-level texture indicators are integrated. An overview of these outcomes metrics is displayed in Table 3 [29].

Advances in Radiomics, AI, and Technical Innovations

Radiomics techniques that extract detailed quantitative features from DCE-MRI have enhanced clinical decision-making. For example, models predicting microvascular invasion in HCC using DCE-MRI radiomic features have accomplished AUCs of 0.868 in the learning phase and 0.857 in confirmation sets, underscoring their diagnostic promise [41]. Although substantial progress has been made in classifying and standardizing radiomic biomarkers, there remains a noticeable lack of emphasis on the careful planning and execution of radiomic studies focused on imaging diagnostic signal breakthrough, while analyzing outcomes, many released investigations exhibit methodological errors or fall short in providing adequate methodological transparency, hindering the reader's ability to contextualize findings [42,43]. Drawing on recent collaborative experiences in radiomics research and peer review roles for journals such as Radiology, key design and statistical considerations have been identified [16]. This decision does not aim to deliver a comprehensive overview of technical radiomic

features such as grayscale level or bin width, which are extensively reviewed elsewhere, nor does it attempt to catalog all possible sources of bias. Instead, the goal is to highlight frequent pitfalls in radiomic study design and propose practical strategies to mitigate them. By doing so, the field can move toward generating robust, reproducible, and clinically relevant outcomes capable of meaningfully advancing patient care [44].

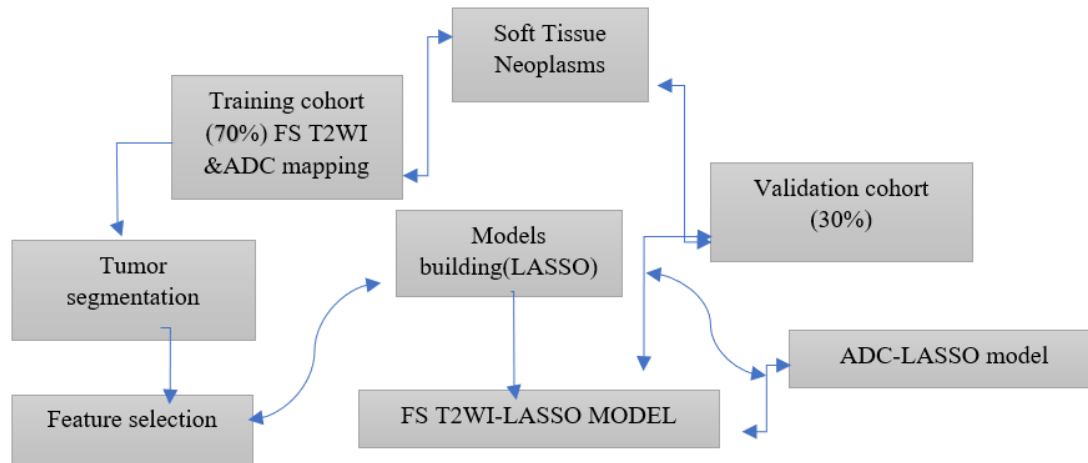


Fig 5: Flowchart of radiomics and machine learning.

Radiomics demands a huge quantity of superior-quality information for assessment. Easily, such databases are not accessible. Most of the existing data collections are retrospective and hence do not have sufficient data on the applicability of outcomes. There is a requirement for prospective data collection. The association between diverse radiomic traits can be acquired by segmentation. Furthermore, the rapid evolution of automated techniques retrieving extensive-scale numerical attributes from medical imaging has led to a significant surge in radiomics-related publications .

Furthermore, the rapid evolution of automated techniques retrieving extensive-scale numerical attributes from medical imaging has led to a significant surge in radiomics-related publications [45]. These studies often aim to leverage combinations of imaging features for tasks such as disease diagnosis, prognosis, therapy planning, or other decision-support functions. Radiomics refers not to the features themselves, ranging from conventional metrics like Hounsfield units to more complex textural and machine-learned parameters [46]. Despite its promise, a critical concern is that only a minor fraction of these measurable visual diagnostics achieve clinical translation. To date, no high-throughput radiomic signature has gained widespread clinical adoption. This underscores the importance of recognizing potential methodological barriers, including variability in study designs. Identifying and overcoming these hidden challenges is essential to realizing the full clinical potential of radiomics [47].

Although its capabilities, radiomics has not yet attained broad clinical incorporation. Moskowitz et al. Note that no high-processing-rate radiomic patterns are presently in standard clinical use. This lack of implementation is mostly credited to irregular confirmation, a lack of normalization, and the existence of unsettled technical and statistical biases.

Moskowitz et al recognize that many radiomic research efforts are subject to structured biases that weaken applicability. Frequent challenges involve bias when imaging elements are also used to determine outcomes, verification bias due to targeted selection of validated cases, and spectrum bias when study cohorts do not represent the wider clinical population. The picking of images to be employed, both for preparation and confirming a radiomics framework, needs to be evaluated. Certain results, such as histologic diagnosis, are merely analyzed for a group of cases, based in part on medical analysis of imaging outcomes. Constraining the research to these patient image results in validation bias (Table 1,) which is a data absence issue that might produce production of sensitivity that are too inflated predictions, of specificity that are too low, or in rare scenarios, lack of capacity in a straightforward manner predict sensitivity and specificity. A distinct study design

has been recommended to prevent this bias, and there are numerous approaches put forward to bias-adjustment ways when validation bias is considered inevitable [48].

Excessive fitting continues to be a major challenge in radiomics simulation. It happens when models are fitted too closely to specific datasets, detecting noise rather than the true signal, thus lowering general reliability. This issue, combined with uncorrected multiple testing where hundreds of features are explored without proper statistical safeguards, frequently inflates performance metrics, as highlighted by Moskowitz et al. Feature values in radiomics are highly sensitive to image acquisition parameters, scanner types, and segmentation approaches. Moskowitz et al. emphasize that even identical features extracted from the same anatomical region can vary significantly across platforms or acquisition protocols, undermining reproducibility and cross-institutional comparability. To ensure clinical relevance and reproducibility, rigorous study design and transparent reporting are essential. As recommended by Moskowitz et al., adherence to guidelines such as STARD for diagnostic accuracy, TRIPOD for prediction modeling, and REMARK for tumor markers can improve the quality of radiomic research and facilitate eventual clinical adoption.

Table 3. Repeated contributors of deviation and Bias in Radiomic studies

Type (Study design)	Description
Spectrum bias (Ransohoff et al.,) [49].	Study are not fully representative of the population of interest Example; model developed using only extreme cases(eg, very sick and/or very healthy individuals)
Verification bias (Begg et al.,1988) [50].	Analysis only includes cases where the outcomes is axcertained, which is nonrepresentative subset of the population of interest Example: Only including patients with biopsies where the decision to biopsy to determined based on imaging.
Incorporation bias (Zhou et al.,2002) [51].	Final result uses data from the images beings examined, Example; Predicting the outcomes from CT images where the outcome is defined by radiologists from CT imaging.
Software variability (Fornacon et al.,2020) [52].	Feature measurement of the same region of interest in the same scan can give different results Example; custom designed attributes, computed on a distinct platform, or with a different version of the same software, can have different values despite compliance with accepted standards.
Operator variability (Pavic et al., 2018) [53].	Manual or semiautomated segmentation affects feature measurement Example Inter-and intraoperator variability exists in manual contours; this variability is also influenced by the disease site and existing clinical contour guidelines .
Bias due to overfitting (Hawkins et al.,2004) [54].	Model captures spurious association in the training data, in addition to assosiation that would be replicated in similar data sets. Example A model captures random variation (Noise) in the training data and appears to perform well but does not work well in independent validation data.
Bias from exclusion of indeterminate or missing feature data (Begg et al.,) [50].	Ignoring images with missing features measurements in analyses might result in to biased assessments of the charecteristics and the algorithmis performance, as well as decreased generalizability of the algorithm .

<p>Optimistic Performance bias (Harrell et al.,1996) [55].</p>	<p>Evaluating the algorithms on the same data that was used to build or optimize the algorithm.</p>
--	---

To overcome these challenges, recent efforts have focused on improving study design, quality control, and transparency in radiomics research. A robust radiomics study must incorporate sound feature selection, appropriate modeling methodology, and comprehensive validation. Feature selection should be data-driven, incorporating dimensionality reduction techniques to eliminate non-robust or redundant variables. Modeling often relies on a single machine learning technique, but the use of multiple algorithms can enhance generalizability. Crucially, the validation process should include discrimination and calibration metrics, supported by bootstrapping or cross-validation to reduce sampling bias [56]. To standardize methodological rigor, the radiomics quality score (RQS) was developed, guiding researchers to report protocols, QA procedures, and justification for model decisions. RQS also encourages full transparency in prediction model development, complementing frameworks like TRIPOD, which mandate complete and unbiased reporting of multi-variable prediction models. These frameworks are essential for reducing bias, improving replicability, and facilitating the clinical adoption of radiomics-based tools [57].

DISCUSSION

(DCE-MRI) Dynamic contrast-enhanced MRI continues to gain traction as a powerful imaging modality for non-invasively assessing liver tumors, offering insights into perfusion dynamics, vascular permeability, and extracellular volume. Its strength lies in the ability to acquire images continuously, often during free-breathing, with motion corrected reconstruction that achieves high temporal resolution typically within 6-second intervals [15]. Commercially available post-processing tools facilitate this process by incorporating motion correction algorithms with adjustable translational and reproducibility [58]. Quantitative pharmacokinetic parameters derived from DCE-MRI, including K_{trans} , K_{ep} , and V_e , serve as critical indicators of tumor behavior and treatment response. These metrics are estimated on a voxel-wise framework utilizing constrained nonlinear modeling methods, often supported by models that account for additional variables such as arterial and venous plasma flow, extracellular volume, and delay times. Such modeling techniques, using Lavenberg-Marquardt optimization, are reinforced with constraints to maintain physiologic plausibility [59].

In clinical settings, these parameters offer significant diagnostic values, with evidence showing that they can detect therapeutic effects, recurrence, or treatment failures earlier than conventional imaging techniques. For example, post-radiotherapy reductions in k_{trans} and V_p have consistently been observed among treatment responders, suggesting a correlation between these perfusion metrics and therapeutic efficacy [60]. Despite these benefits, several challenges hinder DCE-MRI's universal adoption. Tumor heterogeneity, inconsistent imaging follow-ups, and technical complexity can affect parameter reliability [61]. Additionally, achieving diagnostically sufficient image quality can be cumbersome, often requiring repeat contrast-enhanced scans, adding burden to both patients and healthcare workflows. Nevertheless, DCE-MRI remains an essential tool, especially when paired with systematic statistical evaluation and interobserver agreement. Its potential for early response prediction and precision monitoring reaffirms its emerging role in oncology imaging, although alignment and refinement of imaging parameters remain areas for ongoing development [47].

The advanced clinical utility of Dynamic Contrast-enhanced-MRI in liver cancer, upcoming research should target many key areas. Standardization of parameters and acquisition protocols is essential to reassure routine use of DCE-MRI metrics, particularly for distinguishing between liver pathologies like (HCC) hepatocellular carcinoma and (HCA) hepatocellular adenoma. Longitudinal studies tracking DCE-MRI parameter changes over time could offer precious insights into tumor progression and treatment response, supporting the development of predictive models for patients' outcomes. Integrating functional MRI techniques alongside DCE-MRI could enhance spatial mapping of liver function and inform more personalized treatment plans [13]. Technical innovations, including advanced K-space undersampling, golden-angle sampling, and training radiologists without excessive use of contrast agents [12]. There is also growing interest in deep learning frameworks to

improve parameter estimation accuracy and reduce computational demands, thereby enhancing diagnostic confidence [13]. Developing cost-effective solutions, such as streamlined protocols and affordable contrast agents, alongside telemedicine integration protocols, DCE-MRI accessibility, especially in low-resource settings [62]. These research directions aim to enhance both the diagnostic power and clinical practicality of DCE-MRI in liver cancer care.

CONCLUSION

Recent reviews consistently highlight the substantial diagnostic significance of Dynamic Contrast Enhanced Magnetic Resonance Imaging in the diagnosis, observation, and characterization of liver tumors. DCE-MRI has proven more effective than standard methods of imaging modalities in categorizing benign from malignant liver lesions, evaluating microvascular invasion, and assessing treatment response. The quantitative parameters it provides, such as K_{trans} , K_{ep} , and V_e , offer critical insights into tumor vascularity and permeability that supports more informed clinical decision-making. Although challenges like protocols variability, motion, artifacts, and limited standardization remain, the integration of radiomics and artificial intelligence with DCE-MRI is seen as a promising direction for improving diagnostic accuracy and patient outcomes. As ongoing research continues to address these limitations, DCE-MRI is likely to make a highly demanding, vital contribution to personalized liver cancer care.

Ethical Statement

None of the authors have conducted any research on humans or animals for this paper.

Conflicts of Interest

The authors declare no conflicts of interest related to this work.

Data Availability Statement

Since this study did not create or analyse any new data, data sharing is not applicable to this article.

FUNDING

The author(s) declare that no financial support was received for the research, authorship, and/or publication of this article.

Author Contribution Statement

Faizan Farooq: original draft, Review and editing , Mohit Sharma: Supervision, Visualization. Khursheed Ahmed: Conceptualization, Formal Analysis, Srishti Bhardwaj: Formal Analysis and Proofreading.

REFERENCES

1. Shao YY, et al. Lenalidomide as second-line therapy for advanced hepatocellular carcinoma: exploration of biomarkers for treatment efficacy. *Alimentary Pharmacology & Therapeutics*. 2017 Oct;46(8):722-30.
2. Chen BB, Shih TT. DCE-MRI in hepatocellular carcinoma-clinical and therapeutic image biomarker. *World journal of gastroenterology: WJG*. 2014 Mar 28;20(12):3125.
3. Zhang J, et al. Assessment of tumor treatment response using active contrast encoding (ACE)-MRI: Comparison with conventional DCE-MRI. *PLoS One*. 2020 Jun 10;15(6):e0234520.
4. O'Connor JP, Jackson A, et al. DCE-MRI biomarkers in the clinical evaluation of antiangiogenic and vascular disrupting agents. *British journal of cancer*. 2007 Jan;96(2):189-95.
5. Song J, Gu Y, Du T, Liu Q. Analysis of quantitative and semi-quantitative parameters of DCE-MRI in differential diagnosis of benign and malignant cervical tumors. *American Journal of Translational Research*. 2021 Nov 15;13(11):12228.

6. Notley SV, Thacker NA, et al. Reliability of Tumour Classification from Multi-Dimensional DCE-MRI Variables using Data Transformations. arXiv preprint arXiv:2303.10014. 2023 Mar 17.
7. Lee SK, Jee WH, Jung CK, Chung YG. Multiparametric quantitative analysis of tumor perfusion and diffusion with 3T MRI: differentiation between benign and malignant soft tissue tumors. *The British journal of radiology*. 2020 Nov 1;93(1115):20191035.
8. Mourad MA, Higazi MM. MRI prognostic factors of tongue cancer: potential predictors of cervical lymph nodes metastases. *Radiology and Oncology*. 2019 Mar 3;53(1):49
9. Gao A, et al., Applying dynamic contrast-enhanced MRI tracer kinetic models to differentiate benign and malignant soft tissue tumors. *Cancer Imaging*. 2024 May 21;24(1):64.
10. Shao YY, et al. Lenalidomide as second-line therapy for advanced hepatocellular carcinoma: exploration of biomarkers for treatment efficacy. *Alimentary Pharmacology & Therapeutics*. 2017 Oct;46(8):722-30.
11. Yang J, Dong X, et al. Radiomics model of dynamic contrast-enhanced MRI for evaluating vessels encapsulating tumor clusters and microvascular invasion in hepatocellular carcinoma. *Academic Radiology*. 2025 Jan 1;32(1):146-56.
12. Wassenaar NP, et al. Optimizing pseudo-spiral sampling for abdominal DCE MRI using a digital anthropomorphic phantom. *Magnetic Resonance in Medicine*. 2024 Nov;92(5):2051-64.
13. Alareer HS, Taher HJ, Abdullah AD. Dynamic contrast enhanced-MRI and apparent diffusion coefficient quantitation for differentiate hepatocellular carcinoma from hepatocellular adenoma. *Asian Pacific Journal of Cancer Prevention: APJCP*. 2024;25(3):931..
14. Wang H, Guo S. Solitary hypovascular hepatic nodules: comparison and differentiation between peripheral nodular cholangiocarcinoma and atypical liver hemangioma with MRI. *Translational Cancer Research*. 2023 Aug 25;12(9):2308.
15. Chen Y et al., Use of dynamic contrast-enhanced MRI for the early assessment of outcome of CyberKnife stereotactic radiosurgery for patients with spinal metastases. *Clinical Radiology*. 2021 Nov 1;76(11):864-e1.
16. Granata V, Grassi R, et al., La Porta M, Brunese MC, De Muzio F, Ottaiano A. Diagnostic evaluation and ablation treatments assessment in hepatocellular carcinoma. *Infectious Agents and Cancer*. 2021 Jul 19;16(1):53.
17. Minutoli F et al., Effect of granulocyte colony-stimulating factor on bone marrow: evaluation by intravoxel incoherent motion and dynamic contrast-enhanced magnetic resonance imaging. *La radiologia medica*. 2020 Mar;125(3):280-7.
18. Chen BB, Shih TT. DCE-MRI in hepatocellular carcinoma-clinical and therapeutic image biomarker. *World journal of gastroenterology: WJG*. 2014 Mar 28;20(12):3125.
19. Spratt DE, et al. Early magnetic resonance imaging biomarkers to predict local control after high dose stereotactic body radiotherapy for patients with sarcoma spine metastases. *The Spine Journal*. 2016 Mar 1;16(3):291-8.
20. Kransdorf MJ, Jelinek JS , et al. Soft- Tissue masses: diagnosis using MR imaging. *AJR Am J Roentgenol* 1989; 153: 541–
21. van Rijswijk CS, Kunz P, et al. Diffusion-weighted MRI in the characterization of soft-tissue tumors. *Journal of Magnetic Resonance Imaging: An Official Journal of The International Society For Magnetic Resonance In Medicine*. 2002 Mar;15(3):302-7.
22. Wu H, Zhang S, Liang C, Liu H, Liu Y, Mei Y, et al. Intravoxel incoherent motion MRI for the differentiation of benign, intermediate, and malignant solid soft- tissue tumors. *J Magn Reson Imaging* 2017; 46: 1611–8.
23. Liu X, et al., Multi-modality radiomics nomogram based on DCE-MRI and ultrasound images for benign and malignant breast lesion classification. *Frontiers in Oncology*. 2022 Dec 2;12:992509.
24. Chung et al., MRI to differentiate benign from malignant soft-tissue tumours of the extremities: a simplified systematic imaging approach using depth, size and heterogeneity of signal intensity. *The British journal of radiology*. 2012 Oct 1;85(1018):e831-6.
25. Chu S, et al., Holodny AI. Measurement of blood perfusion in spinal metastases with dynamic contrast-enhanced magnetic resonance imaging: evaluation of tumor response to radiation therapy. *Spine*. 2013 Oct 15;38(22):E1418-24.

26. Spratt DE, et al. Early magnetic resonance imaging biomarkers to predict local control after high dose stereotactic body radiotherapy for patients with sarcoma spine metastases. *The Spine Journal*. 2016 Mar 1;16(3):291-8.
27. Kumar KA et al. A pilot study evaluating the use of dynamic contrast-enhanced perfusion MRI to predict local recurrence after radiosurgery on spinal metastases. *Technology in Cancer Research & Treatment*. 2017 Dec;16(6):857-65.
28. Lis E, et al., Dynamic contrast-enhanced magnetic resonance imaging of osseous spine metastasis before and 1 hour after high-dose image-guided radiation therapy. *Neurosurgical focus*. 2017 Jan 1;42(1):E9.
29. Hu P, Chen L, Zhou Z. Machine learning in the differentiation of soft tissue neoplasms: comparison of fat-suppressed T2WI and apparent diffusion coefficient (ADC) features-based models. *Journal of Digital Imaging*. 2021 Oct;34(5):1146-55.
30. Vellayappan AP, et al. Quantifying the changes in the tumour vascular micro-environment in spinal metastases treated with stereotactic body radiotherapy-a single arm prospective study. *Radiology and Oncology*. 2022 Dec 13;56(4):525.
31. Lim HK, Jee WH, et al, incoherent motion diffusion-weighted MR imaging for differentiation of benign and malignant musculoskeletal tumours at 3 T. *The British journal of radiology*. 2018 Feb 1;91(1082):20170636
32. Sigmund EE, et al. Intravoxel incoherent motion imaging of tumor microenvironment in locally advanced breast cancer. *Magnetic resonance in medicine*. 2011 May;65(5):1437-47
33. Feng ST, et al., prediction of microvascular invasion in hepatocellular cancer: a radiomics model using Gd-EOB-DTPA-enhanced MRI. *European radiology*. 2019 Sep 1;29(9):4648-59.
34. Chong HH et al., Multi-scale and multi-parametric radiomics of gadoxetate disodium-enhanced MRI predicts microvascular invasion and outcome in patients with solitary hepatocellular carcinoma ≤ 5 cm. *European Radiology*. 2021 Jul;31(7):4824-38.
35. Qiao M, Liu C, et al. Breast tumor classification based on MRI-US images by disentangling modality features. *IEEE Journal of Biomedical and Health Informatics*. 2022 Jan 4;26(7):3059-67.
36. Lee JH, Yoo GS et al., Diffusion-weighted and dynamic contrast-enhanced magnetic resonance imaging after radiation therapy for bone metastases in patients with hepatocellular carcinoma. *Scientific Reports*. 2021 May 17;11(1):10459.
37. Fotouhi M, et al., Assessment of LI-RADS efficacy in classification of hepatocellular carcinoma and benign liver nodules using DCE-MRI features and machine learning. *European Journal of Radiology Open*. 2023 Dec 1;11:100535.
38. Qiao M, Li C, Suo S, et al. Breast DCE-MRI radiomics: a robust computer-aided system based on reproducible BI-RADS features across the influence of datasets bias and segmentation methods. *International journal of computer assisted radiology and surgery*. 2020 Jun;15(6):921-30
39. Guo R, Lu G, Qin B, Fei B. Ultrasound imaging technologies for breast cancer detection and management: a review. *Ultrasound in medicine & biology*. 2018 Jan 1;44(1):37-70.
40. Pinsky RW, Helvie MA. Mammographic breast density: effect on imaging and breast cancer risk. *Journal of the National Comprehensive Cancer Network*. 2010 Oct 1;8(10):1157-65.
41. Jacobs MA, et al., Benign and malignant breast lesions: diagnosis with multiparametric MR imaging. *Radiology*. 2003 Oct;229(1):225-32.
42. Segal E, Sirlin CB, et al. Decoding global gene expression programs in liver cancer by noninvasive imaging. *Nature biotechnology*. 2007 Jun;25(6):675-80.
43. Zhu Y, et al. Bi-regional dynamic contrast-enhanced MRI for prediction of microvascular invasion in solitary BCLC stage A hepatocellular carcinoma. *Insights into Imaging*. 2024 Jun 18;15(1):149.
44. Ronot M, Nahon P et al. Screening of liver cancer with abbreviated MRI. *Hepatology*. 2023 Aug 1;78(2):670-86..
45. Zwanenburg A, et al. The image biomarker standardization initiative: standardized quantitative radiomics for high-throughput image-based phenotyping. *Radiology*. 2020 May;295(2):328-38.
46. Kessler LG, et al., QIBA Terminology Working Group. The emerging science of quantitative imaging biomarkers terminology and definitions for scientific studies and regulatory submissions. *Statistical methods in medical research*. 2015 Feb;24(1):9-26.

47. Park JE, Kim D et al. Quality of science and reporting of radiomics in oncologic studies: room for improvement according to radiomics quality score and TRIPOD statement. *European radiology*. 2020 Jan;30(1):523-36.
48. Moskowicz CS, et al. Radiomic analysis: study design, statistical analysis, and other bias mitigation strategies. *Radiology*. 2022 Aug;304(2):265-73.
49. Ransohoff DF, Feinstein AR. Problems of spectrum and bias in evaluating the efficacy of diagnostic tests. *N Engl J Med* 1978;299(17):926–930.
50. Begg CB, McNeil BJ. Assessment of radiologic tests: control of bias and other design considerations. *Radiology* 1988;167(2):565–569.
51. Zhou XH, et al. In: *Statistical Methods in Diagnostic Medicine*. New York, NY: Wiley-Interscience, 2002; 73–74.
52. Fornacon-Wood I, Mistry H, Ackermann CJ, et al. Reliability and prognostic value of radiomic features are highly dependent on choice of feature extraction platform. *Eur Radiol* 2020;30(11):6241–6250.
53. Pavic M, Bogowicz M, Würms X, et al. Influence of inter-observer delineation variability on radiomics stability in different tumor sites. *Acta Oncol* 2018;57(8):1070–1074.
54. Hawkins DM, et al. (2004). The problem of overfitting. *Journal of Chemical Information and Computer Sciences*, 44(1), 1–12.
55. Harrell FE Jr, et al. (1996). Multivariable prognostic models: issues in developing models, evaluating assumptions and adequacy, and measuring and reducing errors. *Statistics in Medicine*, 15(4), 361–387
56. Collins GS, et al. (2015). Transparent reporting of a multivariable prediction model for individual prognosis or diagnosis (TRIPOD): the TRIPOD statement. *BMJ*, 350, g7594.
57. Gillies RJ, et al. (2016). Radiomics: images are more than pictures, they are data. *Radiology*, 278(2), 563–577.
58. Tadimalla S, Wang W, et al. Role of functional MRI in liver SBRT: Current use and future directions. *Cancers*. 2022 Nov 28;14(23):5860.
59. Mulyadi R, et al. (2023). Dynamic contrast-enhanced magnetic resonance imaging parameter changes as an early biomarker of tumor responses following radiation therapy in patients with spinal metastases: a systematic review. *Radiation Oncology Journal*, 41(4), 225.
60. Yoon JH, et al. (2022). Simultaneous evaluation of perfusion and morphology using GRASP MRI in hepatic fibrosis. *European Radiology*, 32(1), 34–45.
61. Dejene EM, et al. (2023). Unified Bayesian network for uncertainty quantification of physiological parameters in dynamic contrast enhanced (DCE) MRI of the liver. *Physics in Medicine & Biology*, 68(21), 215018.
62. Morin O, et al. (2018). A deep look into the future of quantitative imaging in oncology: a statement of working principles and proposal for change. *International Journal of Radiation Oncology Biology* Physics**, 102(4), 1074–1082.